

Article

# Effect of Thermal-Electric Cross Coupling on Heat Transport in Nanofluids

Zhanxiao Kang <sup>1,2</sup> and Liqiu Wang <sup>1,2,\*</sup>

<sup>1</sup> Department of Mechanical Engineering, The University of Hong Kong, Hong Kong, China; zxkang@connect.hku.hk

<sup>2</sup> Zhejiang Institute of Research and Innovation, The University of Hong Kong (HKU-ZIRI), Hangzhou 311300, Zhejiang, China

\* Correspondence: lqwang@hku.hk; Tel.: +852-3917-7908

Academic Editor: Mehrdad Massoudi

Received: 23 October 2016; Accepted: 9 January 2017; Published: 19 January 2017

**Abstract:** Nanofluids have an enhanced thermal conductivity compared with their base fluid. Although many mechanisms have been proposed, few of them could give a satisfactory explanation of experimental data. In this study, a mechanism of heat transport enhancement is proposed based on the cross coupling of thermal and electric transports in nanofluids. Nanoparticles are viewed as large molecules which have thermal motion together with the molecules of the base fluid. As the nanoparticles have surface charges, the motion of nanoparticles in the high-temperature region will generate a relatively strong varying electric field through which the motion will be transported to other nanoparticles, leading to a simultaneous temperature rise of low-temperature nanoparticles. The local base fluid will thus be heated up by these nanoparticles through molecular collision. Every nanoparticle could, therefore, be considered as an internal heat source, thereby enhancing the equivalent thermal conductivity significantly. This mechanism qualitatively agrees with many experimental data and is thus of significance in designing and applying nanofluids.

**Keywords:** nanofluids; heat transport enhancement; thermal motion; electric field; thermal-electric cross coupling

## 1. Introduction

Heat transfer occurs nearly everywhere from electric power generation, material processing, air conditioning to the cooling of electronic devices [1–7]. Heat transfer enhancement is becoming increasingly important for energy saving and pollution reduction with the energy crisis and environmental problems becoming severe. In our daily life, heat transfer enhancement also draws much attention, since portable electronic devices are becoming thinner and smaller with increasing functions leading to extremely large thermal loads. Hence, thermal management of these devices is of great importance for their safe and efficient operation. One dominating parameter in heat transfer process is the thermal conductivity of working fluid. Generally, the thermal conductivity of working fluid such as water or oil is small compared with solid particles. For example, the thermal conductivity of copper at room temperature is about 700 times greater than that of water, and about 3000 times greater than that of engine oil [8,9]. As a result, nanofluids, which are dilute suspensions of nano-size particles, have drawn much attention [10–13]. For instance, heat transfer of natural convection could be enhanced with a small volume fraction of nanoparticles [14]. Furthermore, many studies [15–17] showed that the application of nanofluids could enhance the performance of solar power systems.

With a small volume fraction of nanoparticles in base fluid such as 0.01%–5%, the thermal conductivity of the mixture could increase significantly. For example, the thermal conductivity enhancement could reach 10%–60% or even exceed 100% in some situations [18–20]. Eastman et al. [21]

observed 44% and 60% enhancement of thermal conductivity for HE-200 oil-based Cu nanofluid (0.052%) and for water-based CuO nanofluid (5%), respectively. Chopkar et al. [22] reported that the thermal conductivity enhancement for water-based  $\text{Ag}_2\text{Al}$  and  $\text{Al}_2\text{Cu}$  nanofluids could reach 140% and 120%, respectively, with nanoparticle concentration of 1.8%. Generally, various factors such as temperature, base fluid, particle volume fraction, particle material, particle size and particle shape have been found to influence the thermal conductivity enhancement of nanofluids [23–25]. For example, the thermal conductivity increases with increasing temperature [25], and the lower thermal conductivity of based fluid, the higher thermal conductivity enhancement of the mixture [26,27]. The aspect ratio of nanoparticles and their tangling are also found to have a great influence on the thermal conductivity of nanofluids [28]. However, the effects of many factors are inconsistent in different experiments. Some studies indicated that the thermal conductivity of nanofluids increased with decreasing particle size [25,29], while other researchers showed increasing thermal conductivity with the increase of particle size [30,31]. A higher thermal conductivity of nanofluids is commonly observed with a higher thermal conductivity of the nanoparticles [32], while Shima and Philip [33] discovered that the thermal conductivity of nanoparticles did not influence the thermal conductivity enhancement of dilute nanofluids, and the thermal conductivity was solely dependent on the volume fraction of nanoparticles. Furthermore, some studies even showed that the nanoparticle with lower thermal conductivity might yield higher thermal conductivity enhancement of nanofluids [34]. To explain the anomalous enhanced thermal conductivity of nanofluids, several possible mechanisms are proposed [23], such as Brownian motion of nanoparticles, liquid layering at the liquid/particle interface, ballistic nature of heat transport in nanoparticles, and the effect of nanoparticle clustering. Although some studies supported the importance of Brownian motion for the enhanced thermal conductivity of nanofluids [35,36], there are other researchers against it [37,38]. As for the liquid layer at the liquid/particle interface, molecular dynamic simulations [39–42] discovered water density fluctuation near the solid surface representing the liquid layer and could explain the thermal behavior such as temperature jump on the surface, while some studies [43–45] indicated that the liquid layer might not influence the thermal behavior of nanofluids. In addition, Keblinski et al. [44] found that ballistic heat transport still could not explain the anomalous thermal conductivity enhancements either. In terms of the nanoparticle clustering, the studies also show contradictory results. Keblinski et al. [44] denoted that clustering of nanoparticles created paths with low thermal resistance leading to enhanced thermal conductivity, while Evans et al. [46] reported that the nanofluid with clusters showed relatively small thermal conductivity enhancement. Therefore, the mechanism responsible for the enhanced thermal conductivity of nanofluids is still unclear.

In this paper, we propose a thermal-electric cross-coupling mechanism to explain the enhanced heat transport in nanofluids through a microscopic model based on molecular dynamics. As nanoparticles in the base fluid have surface charges, a varying electric field will be generated accompanying the particle thermal motion. In this model, the thermal motion of a nanoparticle in the diffusion layer is simplified as a vibration movement to indicate the effect of the cross coupling between thermal motion and electric field. As the electrostatic force is a long-range force, the thermal motion could be transported to other nanoparticles simultaneously, and then local heat exchange with base fluid will take place via molecular collision. This transport process could be the main reason for heat transport enhancement in nanofluids. As this mechanism could qualitatively explain many experimental results in the literatures, it will not only provide a new strategy to understand the beneath mechanism of the enhanced heat transport, but also be of great importance for the design and application of nanofluids.

## 2. Model of Nanofluids

When nanoparticles are exposed to a fluid, a charged layer will be generated on the surface of the particles, where zeta potential is a parameter characterizing the charge density. Under the action of electrostatic force, ions with charges of the opposite sign will be attracted around the particle, forming

a diffusion layer shown in Figure 1a. In most conditions, the radius of the diffusion layer could reach several hundred nanometers or even several micrometers [47], which is much larger than the radius of nanoparticles. Due to Brownian motion, the nanoparticles move irregularly. To simplify Brownian motion of the nanoparticles, we assume their diffusion layers are immobile, which is reasonable since the diffusion layer is much larger than the nanoparticles and, consequently, when a nanoparticle moves a small distance, its diffusion layer may not have enough time to deform. Hence, the movement of a nanoparticle makes the center of the particle charge deviate from the center of the opposite charge of the diffusion layer. Consequently, the nanoparticle will be pulled back because of electrostatic force. However, when the center of the positive and negative charge overlap again, the nanoparticle will have a non-zero velocity, making it move forward, then it will be pulled back again. Therefore, the nanoparticle will vibrate around the charge center of the diffusion layer under the electrostatic force.

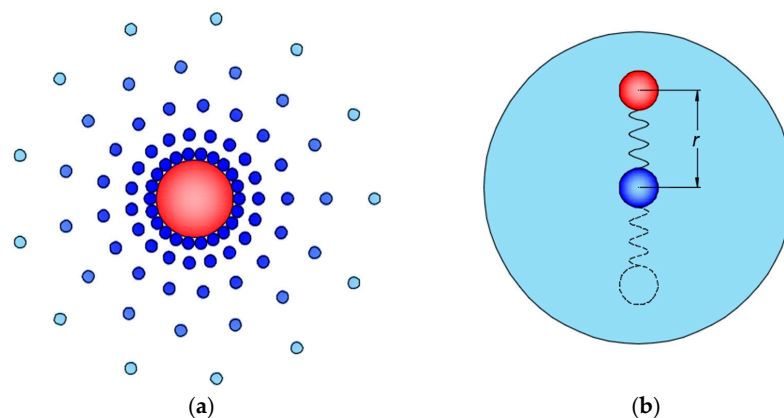


**Figure 1.** (a) Charged nanoparticle with the diffusion layer. The large particle denotes a charged nanoparticle and the small particles indicate the ions with opposite charges; (b) Equivalent vibration model of the nanoparticle. The central particle is a pseudo-particle equivalent to the diffusion layer and the other particle denotes the nanoparticle which vibrates around the pseudo-particle.  $r$  is the relative distance between the nanoparticle and the center of its charged diffusion layer.

In this model, we regard the diffusion layer as a pseudo-charged particle positioned at its center, whose charge quantity is equal to the nanoparticle, but with the opposite sign. Thus, the motion of the nanoparticle could be modeled as a vibration around the pseudo-particle, shown in Figure 1b. In other words, the nanoparticle and the pseudo-particle form an electric dipole, in which the nanoparticle vibrates periodically, with the center of the pseudo-particle being the equilibrium position.

According to electrostatics, the relationship between zeta potential and the corresponding charge quantity could be described approximately based on:

$$\zeta_p \approx \frac{q}{4\pi\epsilon b}; q \approx 4\pi\epsilon b\zeta_p \quad (1)$$

where  $\zeta_p$  is zeta potential,  $q$  is charge quantity,  $\epsilon$  is dielectric constant, and  $b$  is the radius of nanoparticle. The orders of zeta potential and corresponding charge quantity are  $O(10 \text{ mV})$  and  $O(10^{-17} \text{ C})$  respectively [48], where “O” represents magnitude order. The length scale of the diffusion layer could be characterized by Debye length of the electric double layer:

$$\lambda = \sqrt{\frac{\epsilon RT}{F^2 \sum z_i^2 c_i}} \quad (2)$$

where  $\lambda$  is Debye length,  $R$  is the universal gas constant,  $T$  is thermodynamic temperature,  $F$  is Faraday constant,  $z_i$  is chemical valence of species  $i$ , and  $c_i$  is concentration of species  $i$ . The order of  $\lambda$  is  $O(10^{-6} \text{ m})$  in pure water at 300 K, which is larger than the length scale of nanoparticles.

To simplify the model, we assume that all the charges in the diffusion layer distribute homogeneously. Meanwhile, the nanoparticle is considered as a test charge in the diffusion layer. As the whole charge quantity of the diffusion layer equals that of the nanoparticle, the intensity of the electric field in the diffusion layer generated by homogenous ions could be calculated approximately by, according to Equations (1) and (2):

$$E = \frac{1}{4\pi\epsilon} \frac{ql}{\lambda^3} = bF^3 \zeta_p l \left( \frac{\sum z_i^2 c_i}{\epsilon RT} \right)^{3/2} \quad (3)$$

where  $l$  ( $l < \lambda$ ) is the distance to the center of the diffusion layer. As the charges distribute homogeneously in the spherical diffusion layer, the intensity of the electric field, a vector sum, is zero at  $l = 0$  and it increases with the increase of  $l$  when  $l < \lambda$ . The maximum intensity of electric field is the order of  $O(10 \text{ N/C})$  and the corresponding force on the test charge, nanoparticle, is the order of  $O(10^{-16} \text{ N})$ .

Based on thermodynamics, temperature is a macroscopic quantity. It loses its meaning at microscales, especially on the scale of molecules. Temperature characterizes the intensity of the molecular thermal motion, which satisfies the Maxwell–Boltzmann distribution at equilibrium position, according to molecular dynamics. The more intensive the thermal motion, the higher the temperature. Take monatomic ideal gas molecules for an example; the relationship between the average kinetic energy and temperature is given by  $m \cdot v^2 / 2 = 3k \cdot T / 2$ , where  $k$  is Boltzmann constant. For multi-atomic molecules, the energy of thermal motion not only includes translational kinetic energy, but also includes vibration energy and rotational energy. In some solid materials such as crystal, temperature characterizes the average intensity of lattice vibration. Hence, in nanoscale materials like crystal, the temperature gradient is caused by the difference of the lattice vibration energy and the transport of the vibration energy in microscale represents the heat transport in macroscale.

Generally, the length scale of macromolecules could reach 100 nm, which is equivalent to the diameter of nanoparticles, so the nanoparticle and its vibration scale are on the scale of molecules approximately. Consequently, it is reasonable to apply the theory of molecular dynamics to the nanoparticle system and thus the thermal motion of nanoparticles is equivalent to the thermal motion of macromolecules, which is accepted in many literatures [49–52]. In the following, we will adopt the vibration movement of the nanoparticle, denoted in Figure 1b, representing the complicated thermal motion to show the effect of the thermal-electric cross coupling on heat transport in nanofluids. Hence, the temperature has a relationship with the nanoparticle vibration just like the thermal motion of molecules and, thus, the more intensive the vibration, the higher the temperature. In this vibration model, the nanoparticle is assumed to have one vibration freedom. As the kinetic energy and potential energy could transform into each other, we give the average potential energy and kinetic energy of the electric dipole vibration, according to the equipartition theorem:

$$\bar{U} = \frac{1}{2}kT, \quad \bar{E}_k = \frac{1}{2}kT \quad (4)$$

where  $k$  is Boltzmann constant and  $T$  is thermodynamic temperature.

The electric field generated by the charged diffusion layer provides the force to maintain the nanoparticle vibration and the maximum corresponding acceleration is the order of  $O(10^3 \text{ m/s}^2)$ , thus we can obtain the governing equation of the particle vibration based on Equation (3):

$$\frac{d^2 r}{dt^2} + \frac{bF^3 \zeta_p q}{m} \left( \frac{\sum z_i^2 c_i}{\epsilon RT} \right)^{3/2} r = 0; \quad r = 0, \quad \frac{dr}{dt} = \sqrt{\frac{2kT}{m}} \text{ at } t = 0 \quad (5)$$

where  $r$  is relative distance between the nanoparticle and the center of the charged diffusion layer shown in Figure 1b, and  $m$  and  $q$  are the mass and charge quantity of the nanoparticle, respectively. Hence, the solution of Equation (5) is given by:

$$r = \frac{1}{\omega} \sqrt{\frac{2kT}{m}} \sin \omega t \quad (6)$$

where  $\omega = \sqrt{bF^3 \zeta_p q [(\sum z_i^2 c_i) / (\epsilon RT)]^{3/2} / m}$ , which is the angular velocity of the vibration. Therefore, the electric moment of the electric dipole could be obtained:

$$p = qr = \frac{q}{\omega} \sqrt{\frac{2kT}{m}} \sin \omega t \quad (7)$$

As for the whole nanofluid, there are tons of nanoparticles distributed in the base fluid. Every nanoparticle with its charged diffusion layer is equivalent to an electric dipole. In order to model the whole nanofluid, we assume that all the nanoparticles are distributed uniformly and all the directions of the equivalent electric dipoles are the same and perpendicular to the direction of the temperature gradient, which is shown in Figure 2. Furthermore, another assumption is also applied that Brownian motion only results in the vibration of nanoparticles and the equilibrium positions of the nanoparticles remain unchanged.

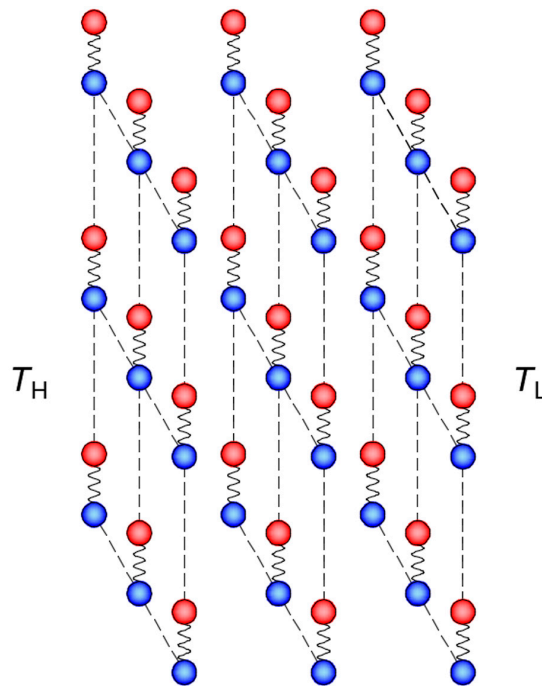


**Figure 2.** Schematic of the model of nanofluid. The equivalent electric dipoles are uniformly distributed in the base fluid and the directions of all dipoles are the same and perpendicular to the direction of the temperature gradient.  $T_H$  and  $T_L$  denote high temperature and low temperature, respectively.

### 3. Cross Coupling of Thermal Motion and Electric Field

#### 3.1. Effect of Electric Field on Heat Transport

According to molecular dynamics, temperature characterizes the intensity of the thermal motion of molecules. In classical heat conduction, the collision of molecules is the main mechanism of heat transport. However, due to the existence of the surface charges of nanoparticles, the electrostatic

force generated by the charged particles may play an important role in heat transport process in nanofluids. In the high-temperature region, the nanoparticles move intensively, while the motion of the nanoparticles is weaker in the low-temperature region. The intensive motion of the charged nanoparticles will generate a strongly varying electric field, which gives a varying electrostatic force on the charged nanoparticles in the low-temperature region. Then, the motion of low-temperature nanoparticles will become intensive simultaneously, which means that the temperature of the nanoparticles becomes higher than the local fluid molecules. As a result, the local fluid will be heated up by the nanoparticles through molecular collision. In this heat transport process, particle–particle interaction is induced by the electrostatic force, while the fluid–fluid and fluid–particle interaction are caused by molecular collision. In other words, the nanoparticles in the low-temperature region are heated up by the high-temperature nanoparticles through varying electrostatic force instantly, and they then transport heat to the local fluid by molecular collision in the low-temperature region, which may be the intrinsic mechanisms of heat transport enhancement in nanofluids.

The nanoparticle with its charged diffusion layer is equivalent to an electric dipole and, to simplify the problem in nanofluids, we take two equivalent dipoles as an example to analyze the cross coupling of thermal motion and electric field, shown in Figure 3. In this two-dipole interaction model,  $L$  is the distance between the two electric dipoles,  $r$  is the relative distance between the nanoparticle and the center of the charged diffusion layer, and  $T_1$  and  $T_2$  ( $T_1 > T_2$ ) are the initial temperature of the two adjacent electric dipoles, respectively. The electric field generated by the high-temperature particle will accelerate the motion of the low-temperature particle and, meanwhile, the electric field generated by the low-temperature particle also influences the motion of the high-temperature particle. In this analysis, we take one step of heat transport from the high-temperature particle to the low-temperature particle as an example to illustrate the effect of electric field on the heat transport process.

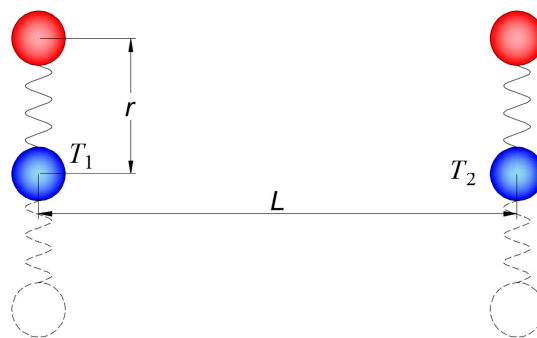


**Figure 3.** Schematic of nanoparticle interaction under the cross coupling of thermal motion and electric field.  $L$  is the distance between the two adjacent electric dipoles,  $r$  is the relative distance between the nanoparticle and the center of its charged diffusion layer and  $T_1$  and  $T_2$  ( $T_1 > T_2$ ) are the initial temperature of the two nanoparticles, respectively.

As  $T_1 > T_2$ , heat will simultaneously transport from the particle with temperature  $T_1$  to the particle with temperature  $T_2$  through the interaction of electric field. According to Equation (7), the electric moment of the electric dipole with temperature  $T_1$  is given by:

$$p_1 = q_1 r = \frac{q_1}{\omega_1} \sqrt{\frac{2kT_1}{m_1}} \sin \omega_1 t; \quad \omega_1 = \sqrt{\frac{b_1 F^3 \zeta_{p1} q_1}{m_1} \left( \frac{\sum z_i^2 c_i}{\epsilon R T_1} \right)^{3/2}} \quad (8)$$

where  $m_1$ ,  $q_1$ ,  $b_1$  and  $\zeta_{p1}$  are the mass, charge quantity, radius and zeta potential of the nanoparticle with temperature  $T_1$ , respectively.

The intensity of the varying electric field, which is generated by the vibration of the electric dipole with temperature  $T_1$ , at the position of electric dipole with temperature  $T_2$  could be calculated via electrostatics:

$$E_1 = -\frac{1}{4\pi\epsilon} \frac{p_1}{L^3} = -\frac{1}{4\pi\epsilon L^3} \frac{q_1}{\omega_1} \sqrt{\frac{2kT_1}{m_1}} \sin \omega_1 t \quad (9)$$

Therefore, the induced motion of the nanoparticle with temperature  $T_2$  because of  $E_1$  is governed by:

$$\frac{d^2 r_2}{dt^2} + \frac{q_2}{4\pi\epsilon m_2 L^3} \frac{q_1}{\omega_1} \sqrt{\frac{2kT_1}{m_1}} \sin \omega_1 t = 0; r_2 = 0 \text{ at } t = 0 \text{ and } t = \tau \quad (10)$$

where  $m_2$  and  $q_2$  are the mass and charge quantity of the nanoparticle with temperature  $T_2$ , respectively, and  $\tau$  is the motion period. The solution of Equation (10) gives:

$$r_2 = \frac{q_1 q_2}{4\pi\epsilon m_2 L^3 \omega_1^3} \sqrt{\frac{2kT_1}{m_1}} \sin \omega_1 t \quad (11)$$

Hence, the vibration frequency induced by the varying electric field is given by:

$$f_2 = \frac{\omega_1}{2\pi} = \frac{1}{2\pi} \sqrt{\frac{b_1 F^3 \zeta_{p1} q_1}{m_1} \left( \frac{\sum z_i^2 c_i}{\epsilon R T_1} \right)^{3/2}} \quad (12)$$

According to Equation (6), the intrinsic vibration of the nanoparticle with temperature  $T_2$  is:

$$r_2^* = \frac{1}{\omega_2} \sqrt{\frac{2kT_2}{m_2}} \sin \omega_2 t; \omega_2 = \sqrt{\frac{b_2 F^3 \zeta_{p2} q_2}{m_2} \left( \frac{\sum z_i^2 c_i}{\epsilon R T_2} \right)^{3/2}} \quad (13)$$

where  $b_2$ ,  $\omega_2$  and  $\zeta_{p2}$  are the radius, angular velocity and zeta potential of the nanoparticle with temperature  $T_2$ , respectively. Thus the intrinsic frequency is governed by the low-temperature nanoparticle and base fluid:

$$f_2^* = \frac{\omega_2}{2\pi} = \frac{1}{2\pi} \sqrt{\frac{b_2 F^3 \zeta_{p2} q_2}{m_2} \left( \frac{\sum z_i^2 c_i}{\epsilon R T_2} \right)^{3/2}} \quad (14)$$

According to the superposition principle, the motion of the nanoparticle with original temperature  $T_2$  could be calculated by, based on Equations (11) and (13):

$$\tilde{r}_2 = \frac{q_1 q_2}{4\pi\epsilon m_2 L^3 \omega_1^3} \sqrt{\frac{2kT_1}{m_1}} \sin \omega_1 t + \frac{1}{\omega_2} \sqrt{\frac{2kT_2}{m_2}} \sin \omega_2 t \quad (15)$$

The velocity of the particle is then given by:

$$v = \frac{d\tilde{r}_2}{dt} = \frac{q_1 q_2}{4\pi\epsilon m_2 L^3 \omega_1^2} \sqrt{\frac{2kT_1}{m_1}} \cos \omega_1 t + \sqrt{\frac{2kT_2}{m_2}} \cos \omega_2 t \quad (16)$$

It should be noted that when the frequency of the induced vibration equals the intrinsic frequency, namely  $\omega_1 = \omega_2$ , resonance will take place and the nanoparticle will have the largest amplitude and velocity, which means that the nanoparticle has the highest temperature. When the resonance takes place, the largest velocity of the nanoparticle is:

$$v_{max} = \frac{q_1 q_2}{4\pi\epsilon m_2 L^3 \omega_1^2} \sqrt{\frac{2kT_1}{m_1}} + \sqrt{\frac{2kT_2}{m_2}} \quad (17)$$

whose order is  $O(10^{-1} \text{ m/s})$  at 300 K. Thus, the energy of the low-temperature nanoparticle is:

$$E_{k2} = \frac{1}{2} m_2 v_{max}^2 = \left( \frac{q_1 q_2}{4\pi\epsilon L^3 \omega_1^2} \right)^2 \frac{kT_1}{m_2 m_1} + \frac{kq_1 q_2}{2\pi\epsilon L^3 \omega_1^2} \sqrt{\frac{T_1 T_2}{m_1 m_2}} + kT_2 = kT_2^* > kT_2 \quad (18)$$

where  $T_2^*$  is the transient temperature of the nanoparticle, which is larger than the local temperature  $T_2$ .

As  $T_2^* > T_2$ , the nanoparticle will transport heat to the local fluid by molecular collision. According to Equations (12) and (14), in the same base fluid, the induced frequency is determined by the nanoparticle with temperature  $T_1$ , while the intrinsic frequency depends on the nanoparticle with temperature  $T_2$ . In actual nanofluids, as the size and shape of the nanoparticles cannot be exactly the same, the induced frequency generated by nanoparticles in the high-temperature region is not unique, but various, and thus there always exist some nanoparticles in the low-temperature region whose intrinsic vibration frequency is equal to one induced frequency. Therefore, resonance is inevitable in nanofluids, leading to the existence of nanoparticles with relatively high temperature surrounding low-temperature base fluid. Consequently, heat will transport from nanoparticle to base fluid by molecular collision. As a result, the heat transport process could be enhanced by the cross coupling of thermal and electric effects, yielding an enhanced thermal conductivity.

### 3.2. Thermal Motion of Magnetic Nanoparticles

If the nanoparticles are magnetic particles, the intensive thermal motion of them in the high-temperature region will generate a strongly varying magnetic induction field, which could give a varying magnetic force on the surrounding magnetic particles. Consequently, the motion of the low-temperature particles will become intensive, leading to a simultaneous temperature rise. Meanwhile, the surrounding molecules of base fluid remain at low temperature, which will be heated up by the relatively high-temperature nanoparticles. As a result, the heat transport process will be enhanced because of the cross coupling of thermal motion and magnetic induction field, which is similar to the cross coupling of thermal motion and electric field.

## 4. Influence Factors of Heat Transport in Nanofluids

The essence of heat transport in microscale is known as the energy transport of thermal motion according to molecular dynamics. The molecules in the high-temperature region have more intensive thermal motion compared with that in the low-temperature region. Hence, the thermal motion will be transported by molecular collision and thus the heat transfer speed is determined by the molecular collision speed. In nanofluids, the electrostatic force is a long-range force compared with the intermolecular force. Thus, unlike the classical heat transport by the collision of molecules, the motion of charged nanoparticles could be transported wherever electric field exists, without the contact of two nanoparticles. As the transport speed of electric field is the speed of light, the transport speed of heat disturbance is also the speed of light. This means that the temperature of a nanoparticle can be influenced by the temperature change of another nanoparticle simultaneously. Therefore, heat transport with charged nanoparticles could be enhanced greatly compared with non-charged molecules. In terms of macroscopic view, we could consider every nanoparticle as an internal heat source, which will greatly enhance the equivalent thermal conductivity.

According to the cross coupling of thermal motion and electric field, the enhanced heat transport is determined by the induced motion, while if the particle charge is neutral, there will be no induced vibration and thus the additional energy caused by induced motion is zero according to



Equation (18). With non-zero particle charge, based on Equation (1), the energy of the low-temperature ( $T_2$ ) nanoparticle, Equation (18), could be rearranged into:

$$E_{k2} = kT_2^* = \frac{kT_1^4}{F^6 L^6} \left( \frac{q_2}{q_1} \right)^2 \frac{m_1}{m_2} \left( \frac{\epsilon R}{\sum z_i^2 c_i} \right)^3 + \frac{2kT_1^2 \sqrt{T_2} q_2}{L^3 F^3} \frac{m_1}{q_1} \left( \frac{m_1}{m_2} \right)^{1/2} \left( \frac{\epsilon R}{\sum z_i^2 c_i} \right)^{3/2} + kT_2 \quad (19)$$

where  $T_2^*$  is the transient temperature of the nanoparticle with original temperature  $T_2$ . Therefore, the temperature difference ( $T_2^* - T_2$ ) between the nanoparticle and the surrounding base fluid is

$$\Delta T = \frac{T_1^4}{F^6 L^6} \left( \frac{q_2}{q_1} \right)^2 \frac{m_1}{m_2} \left( \frac{\epsilon R}{\sum z_i^2 c_i} \right)^3 + \frac{2T_1^2 \sqrt{T_2} q_2}{L^3 F^3} \frac{m_1}{q_1} \left( \frac{m_1}{m_2} \right)^{1/2} \left( \frac{\epsilon R}{\sum z_i^2 c_i} \right)^{3/2} \quad (20)$$

whose order is  $O(10^{-3} \text{ K})$  around room temperature.

On the other hand, if the charged particle is under externally uniform magnetic field, magnetic force, depending on the direction of the magnetic field, will be exerted on the particle. When the direction of the magnetic field is not parallel to the particle velocity, the particle will suffer a magnetic force perpendicular to the particle velocity, and thus part of the vibration energy will transform into rotational kinetic energy, which will lead to a more intensive variation of the electric field. Therefore, an additional temperature rise caused by the rotational motion must be introduced into Equation (20). However, when the direction of the magnetic field is parallel to the particle velocity, the nanoparticle will not suffer magnetic force and thus Equation (20) remains the same.

The cross coupling of thermal and electric effects makes heat transport from high-temperature nanoparticle to low-temperature nanoparticle simultaneously, and, meanwhile, the temperature of the local base fluid is unchanged since the propagation speed of electric field equals the speed of light, which is far too faster than the speed of the energy transport by molecular collision. Then, the preheated nanoparticle will heat up the local fluid leading to a higher equivalent thermal conductivity. Therefore, the temperature difference in Equation (20) is the governing parameter determining the enhancement of heat transport in nanofluids. In other words, the larger the  $\Delta T$ , the larger the equivalent thermal conductivity.

According to Equation (20), the main factors determining the enhancement of equivalent thermal conductivity include temperature, particle charge ratio, particle mass ratio, particle concentration which is inversely proportional to 3 power of  $L$ , and the property of base fluid determined by dielectric constant, ion charges and ion concentrations. Equation (20) shows that the equivalent thermal conductivity increases with the increase in temperature and particle concentration, which qualitatively agrees with the results in many studies [25,29,32,53,54], and part of the experimental data of these literatures are shown in Figure 4. Furthermore, the enhancement of thermal conductivity also depends on the base fluid (agrees with the results in references [26,30]), which determines dielectric constant, ion charges and ion concentrations. It should be noted that the particle mass ratio and particle charge ratio in nanofluids, instead of particle size, affect the equivalent thermal conductivity, which could explain the contradictory experimental results relevant to the influence of particle size [25,29–31]. Meanwhile, Equation (20) also could explain the results in literatures [33,34] that the thermal conductivity of nanoparticles did not influence the thermal conductivity enhancement of dilute nanofluids. Equation (20) is useful in the design of nanofluids. If we need nanofluid with high thermal conductivity enhancement, for example, we can increase the temperature, particle concentration or dielectric constant of the base fluid as well as decrease the ion charges or ion concentrations in base fluid, based on Equation (20).

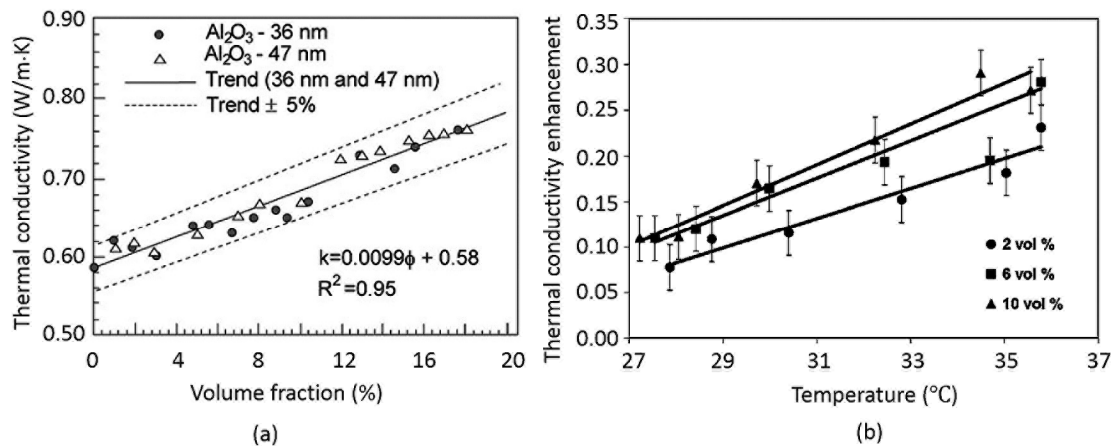


**Figure 4.** Thermal conductivity enhancement with respect to particle volume fraction and temperature. (a) Ambient temperature nanofluid effective thermal conductivity for water-based Al<sub>2</sub>O<sub>3</sub> nanofluid [25]; (b) Thermal conductivity enhancement of Al<sub>2</sub>O<sub>3</sub> in water suspensions against temperature [53]. The thermal conductivity enhancement increases with the increase of particle concentration and temperature, which means that our analysis agrees well with the experimental data qualitatively.

## 5. Concluding Remarks

In nanofluids, a small fraction of nanoparticles in base fluid could enhance the equivalent thermal conductivity significantly. However, the mechanism of heat transport enhancement has not been clear. We proposed a mechanism based on the cross coupling of thermal and electric effects from the aspect of molecular dynamics. As the propagation speed of the electric field equals the speed of light, the thermal motion of the nanoparticle in the high-temperature region could be simultaneously transported to low-temperature nanoparticles, leading to an instant temperature rise of the nanoparticles in the low-temperature region. Then, heat will transport from the preheated nanoparticles to the local base fluid through molecular collision. Thus, each nanoparticle could be considered as an internal heat source, which is the same for magnetic nanoparticles. Hence, the equivalent thermal conductivity will be enhanced. The theoretical analysis shows that the equivalent thermal conductivity of nanofluids increases with increasing temperature and particle concentration. The effect of base fluid is determined by dielectric constant, ion charges and ion concentrations. Particle mass ratio and particle charge ratio in the nanofluids, rather than particle size, influence the thermal conductivity enhancement. As the prediction agrees with the experimental results qualitatively in many literatures and could explain some contradictory results, our proposed mechanism sheds lights on the intrinsic mechanism of the enhanced heat transport by additional nanoparticles, which is of great importance for the design and application of nanofluids.

**Acknowledgments:** The financial support from the Research Grants Council of Hong Kong (GRF 17237316, 17211115, 17207914, and 717613E) and the University of Hong Kong (URC 201511159108, 201411159074 and 201311159187) is gratefully acknowledged. The work is also supported in part by the Zhejiang Provincial, Hangzhou Municipal, and Lin'an County Governments.

**Author Contributions:** Both of the authors have provided substantial contributions to the conception and design of the model, interpretation of the results and writing the article.

**Conflicts of Interest:** The authors declare no conflict of interest.

## Nomenclature

### Symbols

$b$	radius of nanoparticle (m)
$c_i$	concentration of species $i$ (mol/m <sup>3</sup> )
$E$	intensity of the electric field (N/C)
$E_{k2}$	kinetic energy (J)
$\overline{E_k}$	average kinetic energy (J)
$f_2$	induced frequency (Hz)
$f_2^*$	intrinsic frequency (Hz)
$F$	Faraday constant (C/mol)
$k$	Boltzmann constant (J/K)
$l$	distance to the center of diffusion layer (m)
$L$	distance between two nanoparticles (m)
$m$	mass of a nanoparticle (kg)
$p$	electric moment (C·m)
$q$	charge quantity (C)
$r$	vibration displacement (m)
$r_2$	induced vibration displacement (m)
$r_2^*$	intrinsic vibration displacement (m)
$\tilde{r}_2$	vibration displacement (m)
$R$	universal gas constant (J/(mol·K))
$T$	thermodynamic temperature (K)
$T_2^*$	transient temperature (K)
$\Delta T$	temperature difference (K)
$v$	velocity (m/s)
$v_{max}$	maximum velocity (m/s)
$\overline{U}$	average potential energy (J)
$z_i$	chemical valence of species $i$ (-)

### Greek Symbols

$\varepsilon$	dielectric constant (F/m)
$\zeta_p$	zeta potential (V)
$\lambda$	Debye length (m)
$\omega$	angular velocity (rad/s)

### Subscript

1	high-temperature nanoparticle
2	low-temperature nanoparticle

## References

- Goyal, P.; Baredar, P.; Mittal, A.; Siddiqui, A.R. Adsorption refrigeration technology—An overview of theory and its solar energy applications. *Renew. Sustain. Energy Rev.* **2016**, *53*, 1389–1410. [[CrossRef](#)]
- Koroneos, C.; Rovas, D. Exergy analysis of geothermal electricity using the kalina cycle. *Int. J. Exergy* **2013**, *12*, 54–69. [[CrossRef](#)]
- Mills, D. Advances in solar thermal electricity technology. *Sol. Energy* **2004**, *76*, 19–31. [[CrossRef](#)]
- Tian, Y.; Zhao, C.-Y. A review of solar collectors and thermal energy storage in solar thermal applications. *Appl. Energy* **2013**, *104*, 538–553. [[CrossRef](#)]
- Yang, Y.-T.; Wang, Y.-H. Numerical simulation of three-dimensional transient cooling application on a portable electronic device using phase change material. *Int. J. Therm. Sci.* **2012**, *51*, 155–162. [[CrossRef](#)]
- Zhang, Z.; Zhang, N.; Peng, J.; Fang, X.; Gao, X.; Fang, Y. Preparation and thermal energy storage properties of paraffin/expanded graphite composite phase change material. *Appl. Energy* **2012**, *91*, 426–431. [[CrossRef](#)]
- Baby, R.; Balaji, C. Experimental investigations on phase change material based finned heat sinks for electronic equipment cooling. *Int. J. Heat Mass Transf.* **2012**, *55*, 1642–1649. [[CrossRef](#)]
- Eastman, J.A.; Phillpot, S.R.; Choi, S.U.S.; Keblinski, P. Thermal transport in nanofluids. *Annu. Rev. Mater. Res.* **2004**, *34*, 219–246. [[CrossRef](#)]

9. Wang, X.-Q.; Mujumdar, A.S. Heat transfer characteristics of nanofluids: A review. *Int. J. Therm. Sci.* **2007**, *46*, 1–19. [[CrossRef](#)]
10. Ebrahimi-Bajestani, E.; Moghadam, M.C.; Niazmand, H.; Daungthongsuk, W.; Wongwises, S. Experimental and numerical investigation of nanofluids heat transfer characteristics for application in solar heat exchangers. *Int. J. Heat Mass Transf.* **2016**, *92*, 1041–1052. [[CrossRef](#)]
11. Fan, L.-W.; Li, J.-Q.; Li, D.-Y.; Zhang, L.; Yu, Z.-T.; Cen, K.-F. The effect of concentration on transient pool boiling heat transfer of graphene-based aqueous nanofluids. *Int. J. Therm. Sci.* **2015**, *91*, 83–95. [[CrossRef](#)]
12. Raja, M.; Vijayan, R.; Dineshkumar, P.; Venkatesan, M. Review on nanofluids characterization, heat transfer characteristics and applications. *Renew. Sustain. Energy Rev.* **2016**, *64*, 163–173. [[CrossRef](#)]
13. Taylor, R.; Coulombe, S.; Otanicar, T.; Phelan, P.; Gunawan, A.; Lv, W.; Rosengarten, G.; Prasher, R.; Tyagi, H. Small particles, big impacts: A review of the diverse applications of nanofluids. *J. Appl. Phys.* **2013**, *113*, 011301. [[CrossRef](#)]
14. Nnanna, A.G.A. Experimental model of temperature-driven nanofluid. *J. Heat Trans.* **2007**, *129*, 697–704. [[CrossRef](#)]
15. Visconti, P.; Primiceri, P.; Costantini, P.; Colangelo, G.; Cavallera, G. Measurement and control system for thermo-solar plant and performance comparison between traditional and nanofluid solar thermal collectors. *Int. J. Smart Sens. Intell. Syst.* **2016**, *9*, 1220–1242.
16. Milanese, M.; Colangelo, G.; Creti, A.; Lomascolo, M.; Iacobazzi, F.; de Risi, A. Optical absorption measurements of oxide nanoparticles for application as nanofluid in direct absorption solar power systems—Part II: ZnO, CeO<sub>2</sub>, Fe<sub>2</sub>O<sub>3</sub> nanoparticles behavior. *Sol. Energy Mater. Sol. Cells* **2016**, *147*, 321–326. [[CrossRef](#)]
17. Milanese, M.; Colangelo, G.; Creti, A.; Lomascolo, M.; Iacobazzi, F.; de Risi, A. Optical absorption measurements of oxide nanoparticles for application as nanofluid in direct absorption solar power systems—Part I: Water-based nanofluids behavior. *Sol. Energy Mater. Sol. Cells* **2016**, *147*, 315–320. [[CrossRef](#)]
18. Michaelides, E.E. Transport properties of nanofluids. A critical review. *J. Non-Equilib. Thermodyn.* **2013**, *38*, 1–79. [[CrossRef](#)]
19. Murshed, S.M.S.; Leong, K.C.; Yang, C. Thermophysical and electrokinetic properties of nanofluids—A critical review. *Appl. Therm. Eng.* **2008**, *28*, 2109–2125. [[CrossRef](#)]
20. Azmi, W.H.; Sharma, K.V.; Mamat, R.; Najafi, G.; Mohamad, M.S. The enhancement of effective thermal conductivity and effective dynamic viscosity of nanofluids—A review. *Renew. Sustain. Energy Rev.* **2016**, *53*, 1046–1058. [[CrossRef](#)]
21. Eastman, J.; Choi, U.; Li, S.; Thompson, L.; Lee, S. Enhanced thermal conductivity through the development of nanofluids. In Proceedings of the 1996 Fall meeting of the Materials Research Society (MRS), Boston, MA, USA, 2–6 December 1996.
22. Chopkar, M.; Sudarshan, S.; Das, P.; Manna, I. Effect of particle size on thermal conductivity of nanofluid. *Metall. Mater. Trans. A* **2008**, *39*, 1535–1542. [[CrossRef](#)]
23. Angayarkanni, S.A.; Philip, J. Review on thermal properties of nanofluids: Recent developments. *Adv. Colloid Interface Sci.* **2015**, *225*, 146–176. [[CrossRef](#)] [[PubMed](#)]
24. Ozerinc, S.; Kakac, S.; Yazicioglu, A.G. Enhanced thermal conductivity of nanofluids: A state-of-the-art review. *Microfluid. Nanofluid.* **2009**, *8*, 145–170. [[CrossRef](#)]
25. Mintsu, H.A.; Roy, G.; Nguyen, C.T.; Doucet, D. New temperature dependent thermal conductivity data for water-based nanofluids. *Int. J. Therm. Sci.* **2009**, *48*, 363–371. [[CrossRef](#)]
26. Colangelo, G.; Favale, E.; de Risi, A.; Laforgia, D. Results of experimental investigations on the heat conductivity of nanofluids based on diathermic oil for high temperature applications. *Appl. Energy* **2012**, *97*, 828–833. [[CrossRef](#)]
27. Xuan, Y.M.; Li, Q. Heat transfer enhancement of nanofluids. *Int. J. Heat Fluid Flow* **2000**, *21*, 58–64. [[CrossRef](#)]
28. Gu, B.M.; Hou, B.; Lu, Z.X.; Wang, Z.L.; Chen, S.F. Thermal conductivity of nanofluids containing high aspect ratio fillers. *Int. J. Heat Mass Transf.* **2013**, *64*, 108–114. [[CrossRef](#)]
29. Kim, S.H.; Choi, S.R.; Kim, D. Thermal conductivity of metal-oxide nanofluids: Particle size dependence and effect of laser irradiation. *J. Heat Transf.* **2007**, *129*, 298–307. [[CrossRef](#)]
30. Beck, M.P.; Yuan, Y.; Warriar, P.; Teja, A.S. The thermal conductivity of alumina nanofluids in water, ethylene glycol, and ethylene glycol+ water mixtures. *J. Nanopart. Res.* **2010**, *12*, 1469–1477. [[CrossRef](#)]
31. Beck, M.P.; Yuan, Y.; Warriar, P.; Teja, A.S. The thermal conductivity of aqueous nanofluids containing ceria nanoparticles. *J. Appl. Phys.* **2010**, *107*, 066101. [[CrossRef](#)]

32. Hwang, Y.; Ahn, Y.; Shin, H.; Lee, C.; Kim, G.; Park, H.; Lee, J. Investigation on characteristics of thermal conductivity enhancement of nanofluids. *Curr. Appl. Phys.* **2006**, *6*, 1068–1071. [[CrossRef](#)]
33. Shima, P.D.; Philip, J. Role of thermal conductivity of dispersed nanoparticles on heat transfer properties of nanofluid. *Ind. Eng. Chem. Res.* **2014**, *53*, 980–988. [[CrossRef](#)]
34. Sundar, L.S.; Farooqy, M.H.; Sarada, S.N.; Singh, M.K. Experimental thermal conductivity of ethylene glycol and water mixture based low volume concentration of Al<sub>2</sub>O<sub>3</sub> and CuO nanofluids. *Int. Commun. Heat Mass Transf.* **2013**, *41*, 41–46. [[CrossRef](#)]
35. Jang, S.P.; Choi, S.U. Role of brownian motion in the enhanced thermal conductivity of nanofluids. *Appl. Phys. Lett.* **2004**, *84*, 4316–4318. [[CrossRef](#)]
36. Jang, S.P.; Choi, S.U. Effects of various parameters on nanofluid thermal conductivity. *J. Heat Transf.* **2007**, *129*, 617–623. [[CrossRef](#)]
37. Beck, M.P.; Sun, T.; Teja, A.S. The thermal conductivity of alumina nanoparticles dispersed in ethylene glycol. *Fluid Phase Equilib.* **2007**, *260*, 275–278. [[CrossRef](#)]
38. Evans, W.; Fish, J.; Keblinski, P. Role of brownian motion hydrodynamics on nanofluid thermal conductivity. *Appl. Phys. Lett.* **2006**, *88*, 093116. [[CrossRef](#)]
39. Kim, B.H.; Beskok, A.; Cagin, T. Molecular dynamics simulations of thermal resistance at the liquid-solid interface. *J. Chem. Phys.* **2008**, *129*, 174701. [[CrossRef](#)] [[PubMed](#)]
40. Ramos-Alvarado, B.; Kumar, S.; Peterson, G.P. Solid-liquid thermal transport and its relationship with wettability and the interfacial liquid structure. *J. Phys. Chem. Lett.* **2016**, *7*, 3497–3501. [[CrossRef](#)] [[PubMed](#)]
41. Alexeev, D.; Chen, J.; Walther, J.H.; Giapis, K.P.; Angelikopoulos, P.; Koumoutsakos, P. Kapitza resistance between few-layer graphene and water: Liquid layering effects. *Nano Lett.* **2015**, *15*, 5744–5749. [[CrossRef](#)] [[PubMed](#)]
42. Vo, T.Q.; Kim, B. Transport phenomena of water in molecular fluidic channels. *Sci. Rep.* **2016**, *6*, 33881. [[CrossRef](#)] [[PubMed](#)]
43. Iacobazzi, F.; Milanese, M.; Colangelo, G.; Lomascolo, M.; de Risi, A. An explanation of the Al<sub>2</sub>O<sub>3</sub> nanofluid thermal conductivity based on the phonon theory of liquid. *Energy* **2016**, *116*, 786–794. [[CrossRef](#)]
44. Keblinski, P.; Phillpot, S.; Choi, S.; Eastman, J. Mechanisms of heat flow in suspensions of nano-sized particles (nanofluids). *Int. J. Heat Mass Transf.* **2002**, *45*, 855–863. [[CrossRef](#)]
45. Milanese, M.; Iacobazzi, F.; Colangelo, G.; de Risi, A. An investigation of layering phenomenon at the liquid-solid interface in Cu and CuO based nanofluids. *Int. J. Heat Mass Transf.* **2016**, *103*, 564–571. [[CrossRef](#)]
46. Evans, W.; Prasher, R.; Fish, J.; Meakin, P.; Phelan, P.; Keblinski, P. Effect of aggregation and interfacial thermal resistance on thermal conductivity of nanocomposites and colloidal nanofluids. *Int. J. Heat Mass Transf.* **2008**, *51*, 1431–1438. [[CrossRef](#)]
47. Kimura, K.; Takashima, S.; Ohshima, H. Molecular approach to the surface potential estimate of thiolate-modified gold nanoparticles. *J. Phys. Chem. B* **2002**, *106*, 7260–7266. [[CrossRef](#)]
48. Li, X.; Zhu, D.; Wang, X.; Wang, N.; Gao, J.; Li, H. Thermal conductivity enhancement dependent pH and chemical surfactant for Cu-H<sub>2</sub>O nanofluids. *Thermochim. Acta* **2008**, *469*, 98–103. [[CrossRef](#)]
49. Smith, J.S.; Bedrov, D.; Smith, G.D. A molecular dynamics simulation study of nanoparticle interactions in a model polymer-nanoparticle composite. *Compos. Sci. Technol.* **2003**, *63*, 1599–1605. [[CrossRef](#)]
50. Izvekov, S.; Violi, A.; Voth, G.A. Systematic coarse-graining of nanoparticle interactions in molecular dynamics simulation. *J. Phys. Chem. B* **2005**, *109*, 17019–17024. [[CrossRef](#)] [[PubMed](#)]
51. Qin, Y.; Fichthorn, K.A. Molecular-dynamics simulation of forces between nanoparticles in a lennard-jones liquid. *J. Chem. Phys.* **2003**, *119*, 9745–9754. [[CrossRef](#)]
52. Liu, J.; Gao, Y.; Cao, D.; Zhang, L.; Guo, Z. Nanoparticle dispersion and aggregation in polymer nanocomposites: Insights from molecular dynamics simulation. *Langmuir* **2011**, *27*, 7926–7933. [[CrossRef](#)] [[PubMed](#)]
53. Li, C.H.; Peterson, G. Experimental investigation of temperature and volume fraction variations on the effective thermal conductivity of nanoparticle suspensions (nanofluids). *J. Appl. Phys.* **2006**, *99*, 084314. [[CrossRef](#)]
54. Chon, C.H.; Kihm, K.D.; Lee, S.P.; Choi, S.U. Empirical correlation finding the role of temperature and particle size for nanofluid (Al<sub>2</sub>O<sub>3</sub>) thermal conductivity enhancement. *Appl. Phys. Lett.* **2005**, *87*, 3107. [[CrossRef](#)]

